

03,07

## Study of the compressibility of metal cyanamides and the pressure effect on their electronic properties

© D.V. Korabel'nikov, I.A. Fedorov

Kemerovo State University,  
Kemerovo, Russia

E-mail: dkorabelnikov@yandex.ru

Received May 11, 2023

Revised May 11, 2023

Accepted May 26, 2023

Based on the density functional theory, the effect of pressure on the structure and electronic properties of crystalline metal cyanamides  $\text{Zn}(\text{CN}_2)$  and  $\text{NaSc}(\text{CN}_2)_2$  has been studied. The negative linear compressibility of  $\text{Zn}(\text{CN}_2)$  was revealed and its correlation with microscopic changes in the atomic structure under pressure was established. It is shown that  $\text{NaSc}(\text{CN}_2)_2$  has a low compressibility ( $0.2 \text{ TPa}^{-1}$ ) in a direction close to that of cyanamide anions. Based on the quantum topological analysis of the electron density, interatomic interactions were studied and it was found that the Zn-N and Sc-N bonds have a partially covalent character. The band gaps of  $\text{Zn}(\text{CN}_2)$  and  $\text{NaSc}(\text{CN}_2)_2$  at pressures up to 1 GPa have been determined and found to correspond to the UV range of 224–271 nm.

**Keywords:** cyanamide, pressure, compressibility, band gap, electron density.

DOI: 10.61011/PSS.2023.07.56411.81

### 1. Introduction

Zinc cyanamide is a component of environmentally-friendly anticorrosive white pigments [1]. The structure of crystalline zinc cyanamide ( $\text{Zn}(\text{CN}_2)$ ) has been defined fairly recently. The X-ray diffraction method allowed to find that  $\text{Zn}(\text{CN}_2)$  crystal has a tetragonal structure (space group  $I-42d$ ) with the number of formula units  $Z = 8$  [1]. Zinc cations are tetrahedrally coordinated by the nitrogen atoms ( $\text{ZnN}_4$ ), and nitrogen is surrounded by two zinc cations and one carbon atom. Cyanamide anions ( $\text{CN}_2$ ) are almost linear. The first metal cyanamide containing scandium has been synthesized recently. Scandium sodium cyanamide ( $\text{NaSc}(\text{CN}_2)_2$ ) has an orthorhombic structure with symmetry  $Pbcn$  and white color [2]. Sodium and scandium cations have octahedral environment consisting of nitrogen atoms ( $\text{NaN}_6$  and  $\text{ScN}_6$ ). Anions like in  $\text{Zn}(\text{CN}_2)$  are almost linear and contain two crystallographically non-equivalent nitrogen atoms.

Electronic properties of  $\text{Zn}(\text{CN}_2)$  and  $\text{NaSc}(\text{CN}_2)_2$  were studied in [2,3] using theoretical methods (based on the density functional theory (DFT)) and experimental measurements (UV spectroscopy).  $\text{NaSc}(\text{CN}_2)_2$  was found to be a wide-band semiconductor with a band gap width of  $\sim 4 \text{ eV}$ . It is interesting that for hafnium cyanamide ( $\text{Hf}(\text{CN}_2)_2$ ), negative linear compressibility was detected [4]. At the same time, the linear compressibility of crystalline  $\text{Zn}(\text{CN}_2)$  and  $\text{NaSc}(\text{CN}_2)_2$  has not been investigated. Also, by now the dependence of the electronic structure of cyanamide on pressure has not been investigated.

Ab initio calculations are a reliable method of investigation of crystal structure and properties, including high

pressure conditions [5–12]. Results of the ab initio investigation of compressibility and pressure effect on the electronic properties of crystalline  $\text{Zn}(\text{CN}_2)$  and  $\text{NaSc}(\text{CN}_2)_2$  are described herein.

### 2. Calculation method

The ab initio calculations of the atomic and electronic structure were carried out using CRYSTAL software [13]. The calculations used the all-electron pob-TZVP-rev2 atomic orbital basis sets based on pob-TZVP basis sets corrected to minimize their superposition error [14]. PBE exchange-correlation functional was used for geometry optimization [15]. For band gap calculation, B3LYP hybrid functional was used [16], which allows to solve the problem of underestimation existing within the standard functionals. The ab initio determination of the crystalline structure allowed the relaxation of all lattice atoms and constant according to BFGS algorithm [17]. Convergence with respect to energy was better than  $10^{-7} \text{ eV}$ . For elastic constant calculation, standard ELASTCON procedure [13,18] with default parameters was used. Dependence of linear compressibility on direction was visualized using ELATE [19]. Chemical bonding was studied on the basis of QTAIM quantum theory [20].

### 3. Results and discussion

The calculations for  $\text{Zn}(\text{CN}_2)$  and  $\text{NaSc}(\text{CN}_2)_2$  provided the lattice constants (Table 1), which differ from the experimental values [1,2] by less than 1%.

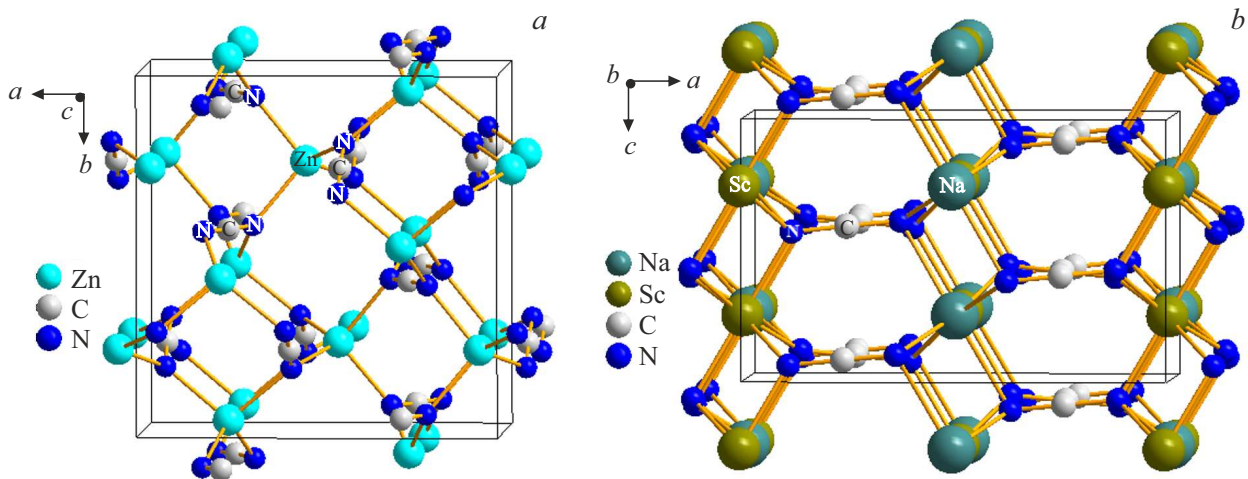


**Figure 1.** Zn(CN<sub>2</sub>) and NaSc(CN<sub>2</sub>)<sub>2</sub> crystal structure.

Crystalline zinc cyanamide and scandium sodium cyanamide have a framework structure where metal cations are bound with the nitrogen atoms of adjacent anions (Figure 1). In NaSc(CN<sub>2</sub>)<sub>2</sub>, cyanamide anions are oriented close to the *a* axis (angle  $\sim 10^\circ$ ).

To study interatomic interactions, topological quantum analysis of the electronic density [20–24] in Zn(CN<sub>2</sub>) and NaSc(CN<sub>2</sub>)<sub>2</sub> was carried out. Whilst *f*-functions were not included in the basis sets. As a result, the presence of binding interactions Zn-N, Na-N, Sc-N between metal cations and cyanamide anions as well as C-N bonds inside anions. Electronic density  $\rho_c$  and Laplacian  $\Delta\rho_c$  in critical points of Zn-N bonds were 0.08 and 0.3 a.u., respectively. Energy density  $H_c$  for Zn-N bonds has a negative value ( $-0.017$  a.u.), which shows that anion-cation interactions in Zn(CN<sub>2</sub>) are partially covalent. Interaction energy Zn-N calculated according to [25] is equal to 144 kJ/mol. Electronic density  $\rho_c$  and energy for Sc-N bonds also have distinctive values 0.06 a.u. and 91 kJ/mol, respectively. Negative energy density ( $-0.008$  a.u.) suggests the presence of a covalent component for Sc-N bonds. For Na-N bonds, the electronic density  $\rho_c$  (0.015 a.u.) and energy (15 kJ/mol) are comparatively low. However, the energy density  $H_c$  for Na-N bonds is positive (0.004 a.u.) indicating their electrostatic nature (closed shell type interactions). Instead, for C-N bonds, the electronic density in the critical points is relatively high ( $\sim 0.4$  a.u.), and Laplacian  $\Delta\rho_c$  is negative ( $-1.2$  a.u.). Thus, in anions between the carbon and nitrogen atoms, covalent bonds exist, which explains low deformation of anions in compression (lower than 0.1%).

Figure 2 demonstrates the calculated dependences on pressure for lattice constants and cell volume of Zn(CN<sub>2</sub>) and NaSc(CN<sub>2</sub>)<sub>2</sub>. It can be seen that for zinc cyanamide with the increasing external pressure, *a* decreases, while the negative linear compressibility takes place along the *c* axis. Also, it can be seen that NaSc(CN<sub>2</sub>)<sub>2</sub> in the *a* axis direction is almost incompressible. This may be associated

**Table 1.** The calculated and experimental lattice constants *a*, *b*, *c* (Å) and the lattice cell volume *V* (Å<sup>3</sup>) of metal cyanamides

Cyanamide	Method	<i>a</i>	<i>b</i>	<i>c</i>	<i>V</i>
Zn(CN <sub>2</sub> )	Calculation	8.883	8.883	5.463	431.1
	exp. [1]	8.805	8.805	5.433	421.2
NaSc(CN <sub>2</sub> ) <sub>2</sub>	Calculation	9.728	7.160	5.970	415.8
	exp. [2]	9.631	7.103	5.952	407.2

with the fact that the *a* axis direction is close to the orientation of cyanamide anions, thus, to the direction of strong bonds C-N.

Instead, in the *b* and *c* axes, distinctive compressibility of NaSc(CN<sub>2</sub>)<sub>2</sub> takes place. Thus, Zn(CN<sub>2</sub>) and NaSc(CN<sub>2</sub>)<sub>2</sub> exhibit strong compressibility anisotropy.

To explore the nature of the negative linear compressibility of Zn(CN<sub>2</sub>), baric dependences of the angle  $\varphi$  between anions and cations ( $\angle(\text{N-Zn-N})$ ) and of the angle  $\alpha$  between anions and the *c* axis were calculated (Figure 3).

As can be seen on Figure 3, the angle  $\varphi$  increases by  $\sim 1.6^\circ$ , while the angle  $\alpha$  decreases by  $\sim 0.5^\circ$ , when the pressure increases by 1 GPa. As a result, the distances between the anions and their dimensions along the *c* axis increase by 0.02 Å and 0.005 Å, respectively. Thus, the negative compressibility occurs in the *c* axis direction.

Next, elastic constants of Zn(CN<sub>2</sub>) and NaSc(CN<sub>2</sub>)<sub>2</sub> (in brackets) were calculated herein:  $C_{11} = 76.8$  (270),  $C_{22} = 76.8$  (80.9),  $C_{33} = 243$  (98.6),  $C_{44} = 23.0$  (30.4),  $C_{55} = 23.0$  (20.8),  $C_{66} = 22.6$  (17.9),  $C_{12} = 46.9$  (62.2),  $C_{13} = 93.3$  (56.2),  $C_{23} = 93.3$  (36.8) GPa. Mechanical stability criteria (Born criteria) [26] are met for Zn(CN<sub>2</sub>) and NaSc(CN<sub>2</sub>)<sub>2</sub> crystals.

Figure 4 shows dependences of linear compressibility on direction for Zn(CN<sub>2</sub>) and NaSc(CN<sub>2</sub>)<sub>2</sub>.

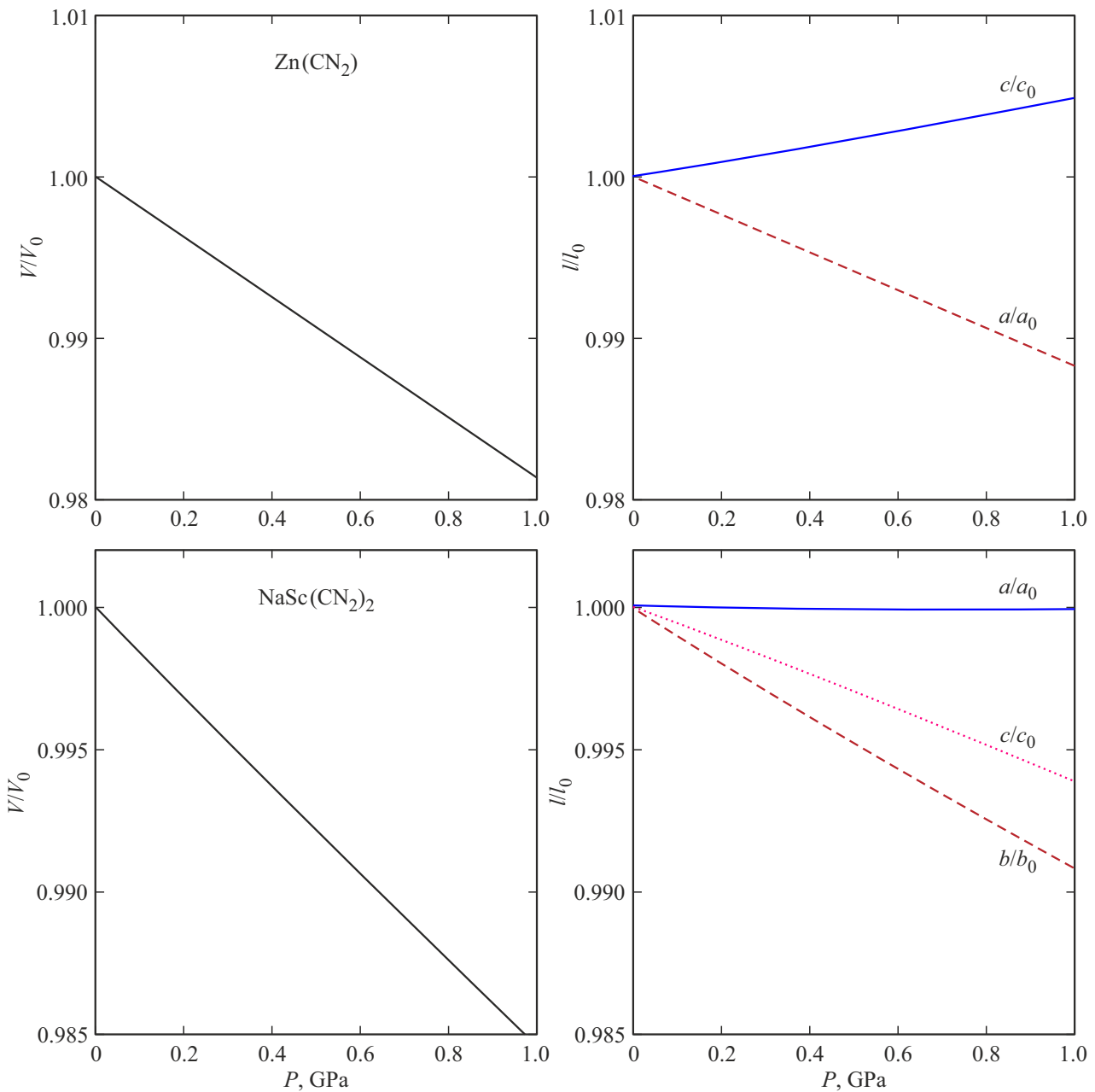


**Figure 2.** Baric dependences of relative volume  $V/V_0$  and lattice constants  $l/l_0$  for  $\text{Zn}(\text{CN}_2)$  and  $\text{NaSc}(\text{CN}_2)_2$ .

Linear compressibilities of  $\text{Zn}(\text{CN}_2)$  and  $\text{NaSc}(\text{CN}_2)_2$  along the crystallographic axes calculated using the elastic constants are listed in Table 2.

Strong compressibility anisotropy of  $\text{Zn}(\text{CN}_2)$  and  $\text{NaSc}(\text{CN}_2)_2$  (in brackets) quantitatively characterizes the relations between compressibilities along the crystallographic axes which have the following values:

$$\beta_c/\beta_b = -0.4(0.7), \quad \beta_c/\beta_a = -0.4(33),$$

$$\beta_b/\beta_a = 1.0(46).$$

Moreover, Table 2 shows the compression bulk modulus, Young's modulus, shear modulus and Poisson's ratio

**Table 2.** Linear compressibilities  $\beta_l$  ( $\text{TPa}^{-1}$ ), bulk modulus  $B$ , Young's modulus  $E$ , shear modulus  $G$  (in GPa) and Poisson's ratio  $\mu$  for  $\text{Zn}(\text{CN}_2)$  and  $\text{NaSc}(\text{CN}_2)_2$

Cyanamide	$\beta_a$	$\beta_b$	$\beta_c$	$B$	$E$	$G$	$\mu$
$\text{Zn}(\text{CN}_2)$	11.8	11.8	-5.0	74.7	61.5	22.6	0.36
$\text{NaSc}(\text{CN}_2)_2$	0.2	9.2	6.6	73.5	78.2	29.6	0.32

calculated in the Voigt–Reuss–Hill approximation [27]. The plastic behavior of crystals is known to be observed

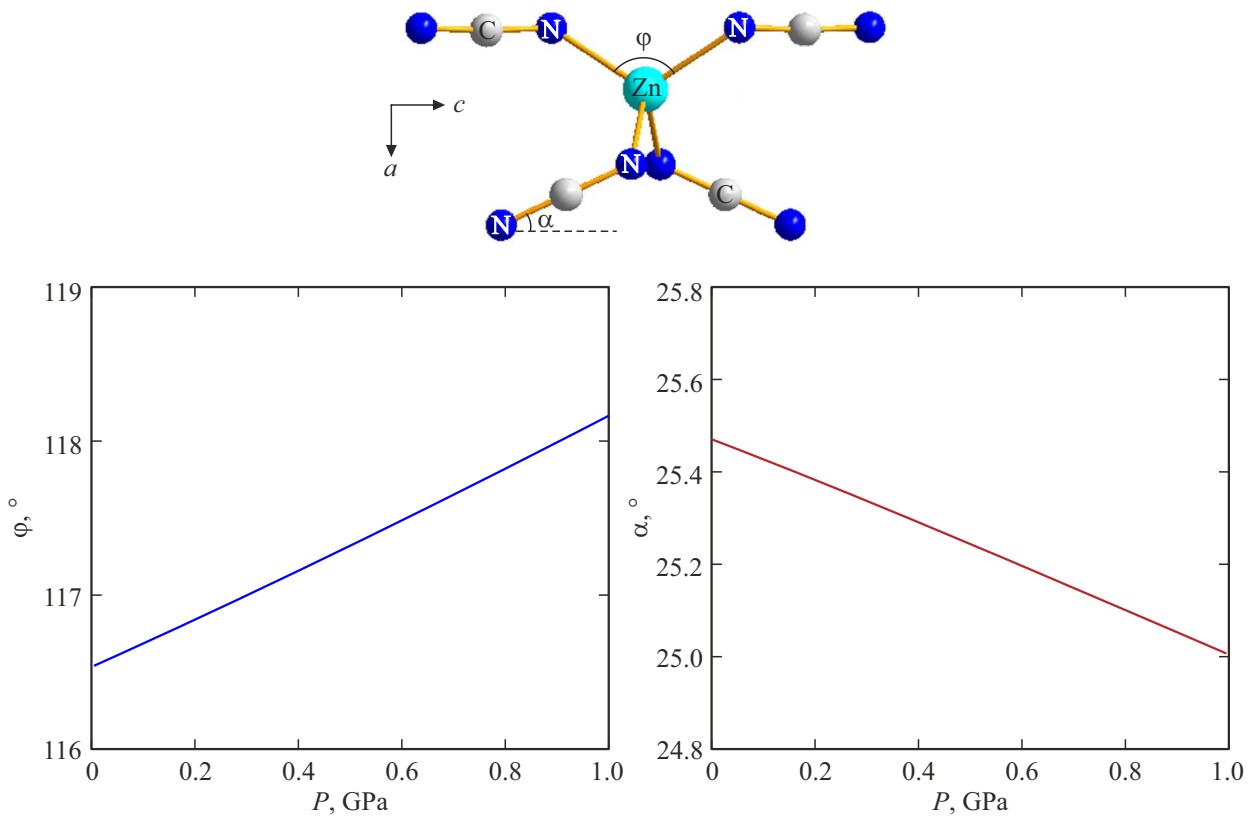


**Figure 3.** Projection of  $Zn(CN_2)$  structure fragment and dependences of angles  $\alpha$  and  $\varphi$  on pressure.

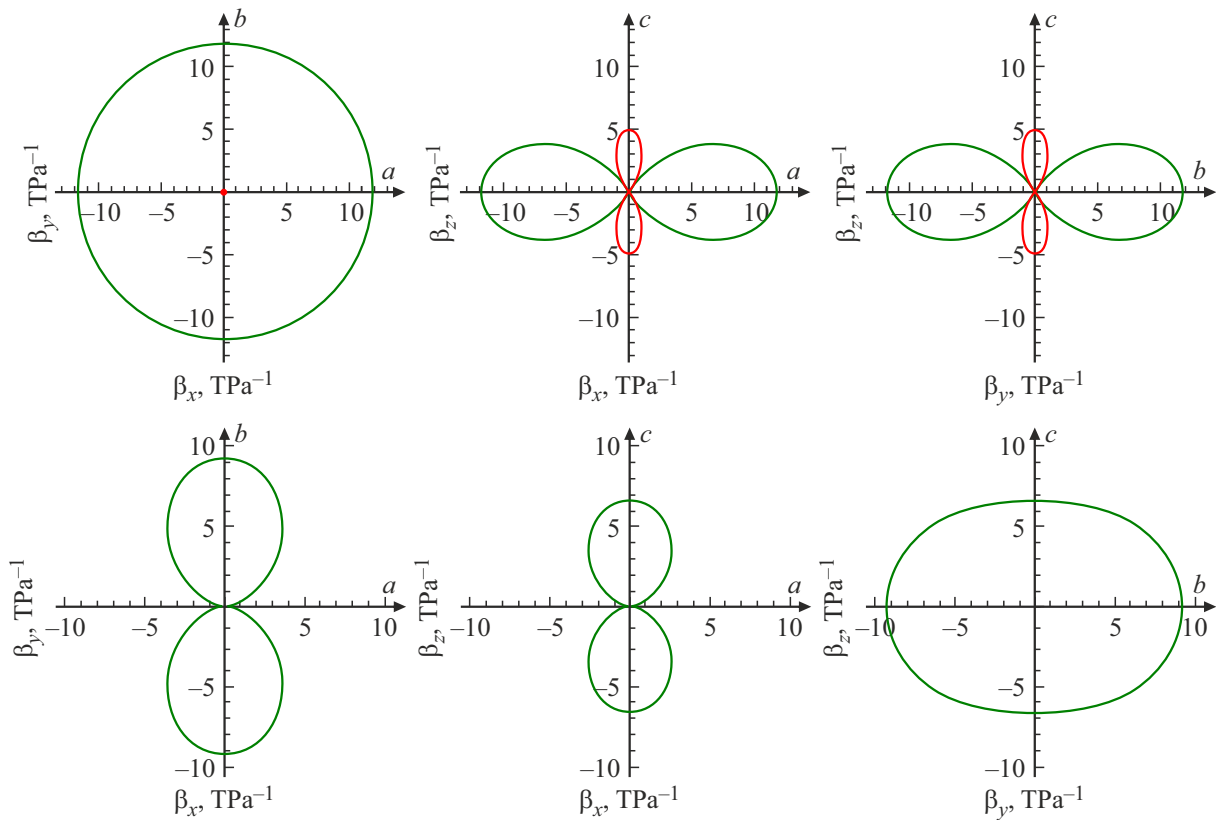


**Figure 4.** Dependences on direction for linear compressibility of  $Zn(CN_2)$  (upper part of the illustration) and  $NaSc(CN_2)_2$  (lower part of the illustration) in various planes.

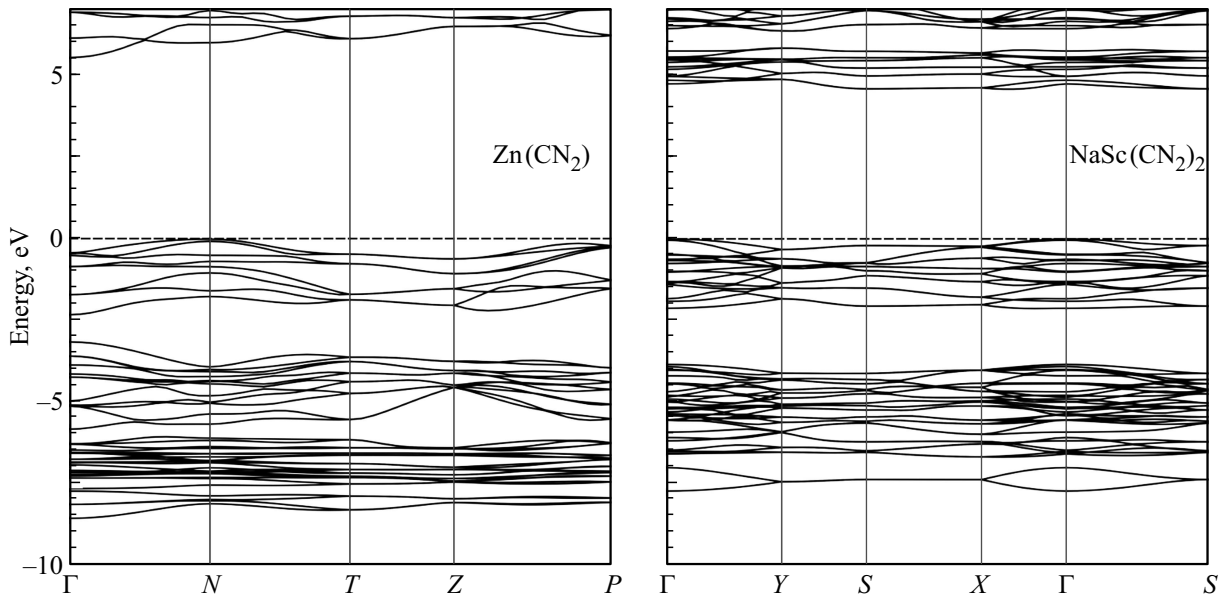


Figure 5.  $\text{Zn}(\text{CN}_2)$  and  $\text{NaSc}(\text{CN}_2)_2$  band structure.

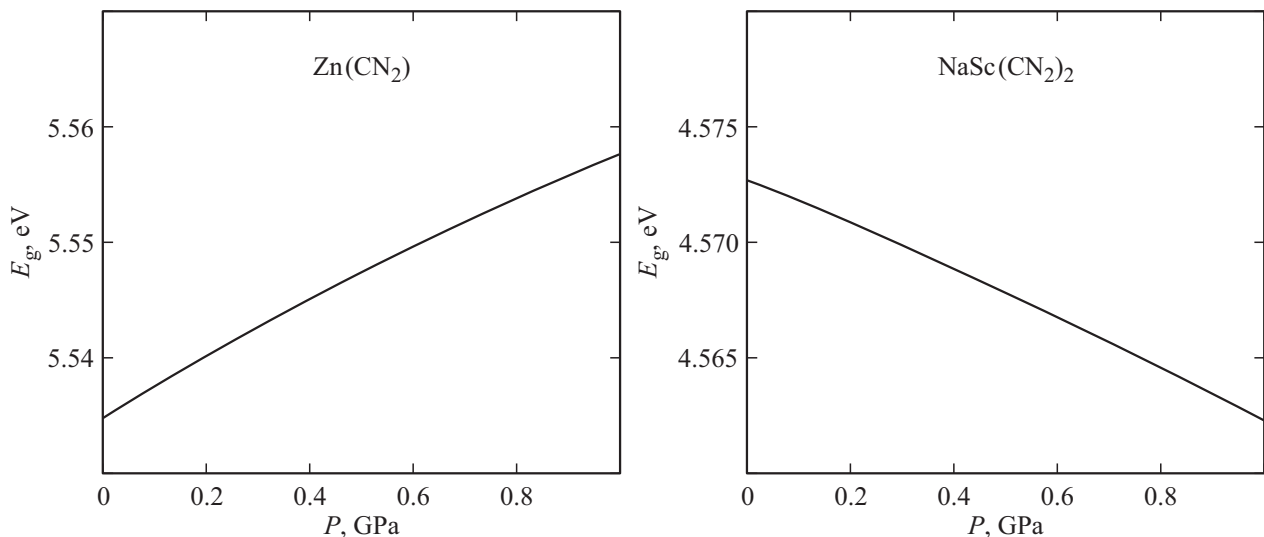


Figure 6. Baric dependences on the band gap of  $\text{Zn}(\text{CN}_2)$  and  $\text{NaSc}(\text{CN}_2)_2$ .

when  $B/G > 1.75$  [28,29]. For  $\text{Zn}(\text{CN}_2)$  and  $\text{NaSc}(\text{CN}_2)_2$ , the relation between the compression and shear moduli  $B/G = 3.3$  (2.5) indicates their plasticity.

$\text{Zn}(\text{CN}_2)$  and  $\text{NaSc}(\text{CN}_2)_2$  band structures are shown in Figure 5. High symmetry points of the Brillouin band have the following coordinates in terms of reciprocal lattice vectors:  $\Gamma$  (0, 0, 0), N (0, 0.5, 0), T (0, 0, 0.5), Z (−0.5, 0.5, 0.5), P (0.25, 0.25, 0.25), Y (0, 0.5, 0), S (0.5, 0.5, 0) and X (0.5, 0, 0). The energy of the highest occupied states is set to zero.

The top of  $\text{Zn}(\text{CN}_2)$  valence band is implemented in point N, while the conduction band bottom corresponds to point  $\Gamma$ . On the other hand, the maximum of  $\text{NaSc}(\text{CN}_2)_2$  valence band is implemented in point  $\Gamma$ .

The bottom unoccupied states correspond to the point on  $\Gamma$ -X line and competing minima are implemented in points S and X. Thus, the band gap of  $\text{Zn}(\text{CN}_2)$  (5.53 eV) and  $\text{NaSc}(\text{CN}_2)_2$  (4.57 eV) is indirect and the absorption edge is defined by indirect transitions. The band gap of  $\text{NaSc}(\text{CN}_2)_2$  calculated herein agrees with its white color and experimental value 4.2 eV [2], which characterizes this material as a wide-band semiconductor. The upper valence bands of  $\text{Zn}(\text{CN}_2)$  and  $\text{NaSc}(\text{CN}_2)_2$  correspond primarily to the nitrogen electron states. Bottom unoccupied bands of  $\text{Zn}(\text{CN}_2)$  are formed as a result of hybridization of electronic states of carbon and nitrogen atoms, while bottom unoccupied bands of  $\text{NaSc}(\text{CN}_2)_2$  correspond to the scandium cation states.

The external pressure is an important tool for modification of the electronic properties of materials [30]. Since crystals with low and negative linear compressibility may be potentially used in highly sensitive optical pressure sensors, it is important to study the baric dependence of the band gap of  $\text{Zn}(\text{CN}_2)$  and  $\text{NaSc}(\text{CN}_2)_2$  (Figure 6).

For  $\text{Zn}(\text{CN}_2)$ , the band gap width grows by 0.023 eV (0.4%), while for  $\text{NaSc}(\text{CN}_2)_2$ , it declines by 0.01 eV (0.2%) with the increasing external pressure from 0 to 1 GPa. Thus, displacement of the absorption edge of  $\text{Zn}(\text{CN}_2)$  and  $\text{NaSc}(\text{CN}_2)_2$  with the growing pressure towards higher and lower energies, respectively, may be predicted. At the same time, the band gap width of  $E_g$  remains indirect and allows optical transparency of  $\text{Zn}(\text{CN}_2)$  and  $\text{NaSc}(\text{CN}_2)_2$  in the visible range (1.6–3.2 eV). Energy of Zn-N (Sc-N) bonds and electronic density in the critical points increase by 3.8 (2.4) and 2.4 (1.7)%, respectively, when the pressure increases up to 1 GPa. The electronic density  $\rho_c$  for C-N bonds increases by 0.25%.

## 4. Conclusion

Results of the ab initio investigation of compressibility anisotropy and pressure effect on the electronic properties of crystalline  $\text{Zn}(\text{CN}_2)$  and  $\text{NaSc}(\text{CN}_2)_2$  are described herein. Deviations of calculated lattice constants from experimental ones were lower than 1%. Elastic constants, band structures, moduli of elasticity, baric dependences of structural parameters and band gaps of cyanamides were calculated.

Negative linear compressibility  $\text{Zn}(\text{CN}_2)$  was revealed for the axis along which the distance between anions and anion sizes increase due to the increasing angle between anions and cation ( $\angle(\text{N-Zn-N})$ ) and by anion rotation with the growing pressure. Dependences of linear compressibility on direction were plotted for the first time and linear compressibilities were also determined along the crystallographic axes of  $\text{Zn}(\text{CN}_2)$  and  $\text{NaSc}(\text{CN}_2)_2$ . It was shown that  $\text{NaSc}(\text{CN}_2)_2$  is almost incompressible in the direction close to the direction of C-N bonds in anions.

Interatomic interactions in  $\text{Zn}(\text{CN}_2)$  and  $\text{NaSc}(\text{CN}_2)_2$  were studied by the topological quantum analysis of the electronic density. Energies of the binding interactions Zn-N, Na-N, Sc-N between metal cations and cyanamide anions were calculated. Zn-N and Sc-N bonds are of partially covalent nature, while Na-N bonds are associated with the closed shell type electrostatic interactions. In the anions between carbon and nitrogen atoms, covalent bonds exist. The energy of Zn-N, Sc-N bonds and the electronic density in the critical points of Zn-N, Sc-N and C-N bonds increase with the increasing external pressure.

Band gap widths of  $\text{Zn}(\text{CN}_2)$  and  $\text{NaSc}(\text{CN}_2)_2$  are indirect and meet the range 4.57–5.53 eV (224–271 nm) that corresponds to wide-band semiconductors. Upper valence and lower unoccupied bands of zinc cyanamide correspond to the anionic states, while the lower unoccupied

bands of  $\text{NaSc}(\text{CN}_2)_2$  correspond to the scandium cation states. Calculations using the hybrid functional showed that the band gap of  $\text{Zn}(\text{CN}_2)$  increases with the increasing external pressure. For  $\text{NaSc}(\text{CN}_2)_2$ , instead, the external pressure causes a decrease in the band gap.

## Acknowledgments

Calculations were performed by the Center of Collective Use „High-performance parallel computations“ of KemSU ([icp.kemsu.ru](http://icp.kemsu.ru)).

## Funding

The study was supported by a grant of the Russian Science Foundation and Kemerovo Region —Kuzbass, project № 22-22-20026. <https://rscf.ru/project/22-22-20026/> (<https://rscf.ru/en/project/22-22-20026/>).

## Conflict of interest

The authors declare that they have no conflict of interest.

## References

- [1] M. Becker, M. Jansen. *Acta Cryst. C.* **57**, 347 (2001).
- [2] A. Corkett, R. Dronskowski, K. Chen. *Eur. J. Inorg. Chem.* **2020**, 2596 (2020).
- [3] Yu.M. Basalae, A.M. Emelyanova, A.V. Sidorova. *J. Struct. Chem.* **59**, 1761 (2018).
- [4] K. Dolabdjian, A. Kobald, C.P. Romao, H-J. Meyer. *Dalton Trans.* **47**, 10249 (2018).
- [5] A.D. Becke. *J. Chem. Phys.* **140**, 18A301 (2014).
- [6] A.R. Oganov, C.J. Pickard, Q. Zhu, R.J. Needs. *Nature. Rev. Mater.* **4**, 331 (2019).
- [7] E. Zurek, W. Grochala. *Phys. Chem. Chem. Phys.* **17**, 2917 (2015).
- [8] D. V. Korabel'nikov, Yu. N. Zhuravlev. *J. Phys. Chem. Solids.* **87**, 38 (2015).
- [9] D.V. Korabel'nikov, Yu.N. Zhuravlev. *Phys. Solid State.* **59**, 254 (2017).
- [10] I.A. Fedorov. *Comput. Mater. Sci.* **139**, 252 (2017).
- [11] D.V. Korabel'nikov, I.A. Fedorov. *Phys. Solid State.* **64**, 1488 (2022).
- [12] D.V. Korabel'nikov, Yu.N. Zhuravlev. *J. Phys. Chem. A.* **121**, 6481 (2017).
- [13] R. Dovesi, R. Orlando, A. Erba, C.M. Zicovich-Wilson, B. Civalleri, S. Casassa, L. Maschio, M. Ferrabone, M. De La Pierre, P. D'Arco, Y. Noel, M. Causa, M. Rerat, B. Kirtman. *Int. J. Quantum Chem.* **114**, 1287 (2014).
- [14] D. Vilela Oliveira, J. Laun, M.F. Peintinger, T. Bredow. *J. Comput. Chem.* **40**, 2364 (2019).
- [15] J.P. Perdew, K. Burke, M. Ernzerhof. *Phys. Rev. Lett.* **77**, 3865 (1996).
- [16] A.D. Becke. *J. Chem. Phys.* **98**, 5648 (1993).
- [17] C.G. Broyden. *J. Appl. Math.* **6**, 222 (1970).
- [18] W.F. Perger, J. Criswell, B. Civalleri, R. Dovesi. *Comput. Phys. Commun.* **180**, 1753 (2009).
- [19] R. Gaillac, P. Pullumbi, F-X. Coudert. *J. Phys. Condens. Matter.* **28**, 275201 (2016).

- [20] R.F.W. Bader. Chem. Rev. **91**, 893 (1991).
- [21] C. Gatti. Z. Kristallogr. **220**, 399 (2005).
- [22] V.G. Tsirelson. Recent Advances in Quantum Theory of Atoms in Molecules. Weinheim: Wiley-VCH (2007).
- [23] E.A. Zhurova, A.I. Stash, V.G. Tsirelson, V.V. Zhurov, E.V. Bartashevich, V.A. Potemkin, A.A. Pinkerton. J. Am. Chem. Soc. **128**, 14728 (2006).
- [24] D.V. Korabel'nikov, Yu.N. Zhuravlev. RSC Advances. **9**, 12020 (2019).
- [25] A.O. Borissova, A.A. Korlyukov, M.Y. Antipin, K.A. Lyssenko. J. Phys. Chem. A. **112**, 11519 (2008).
- [26] F. Mouhat, F-X. Coudert. Phys. Rev. B. **90**, 224104 (2014).
- [27] R. Hill. Proc. Phys. Soc. Sect. A. **65**, 349 (1952).
- [28] S.F. Pugh. Philos. Mag. **45**, 823 (1954).
- [29] S. Masys, V. Jonauskas. Comput. Mater. Sci. **108**, 153 (2015).
- [30] D.V. Korabel'nikov, Yu.N. Zhuravlev. Mater. Sci. Eng. B. **293**, 116468 (2023).

*Translated by Ego Translating*